

Modelling of reversible novolac type phenol-formaldehyde polymerization

Anil Kumar*, Santosh K. Gupta and Birendra Kumar

Department of Chemical Engineering, Indian Institute of Technology, Kanpur-208016, India

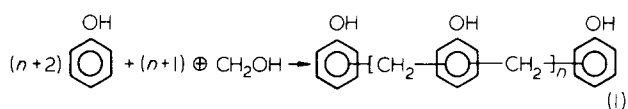
(Received 15 January 1982; revised 7 April 1982)

The reversible polymerization of acid-catalysed phenol and formaldehyde has been modelled through the use of five species A to E. There are two possible mechanisms for the reverse reaction of the polymer formation based upon which two possible kinetic models (1 and 2) have been proposed. These two models arise because during the reverse reaction between these species and water, two possible routes can occur. It has been shown analytically that both these kinetic models would yield identical concentrations of A to E in the reaction mass; only an uncertainty in predicting concentrations of formaldehyde and bound CH_2OH exists. Thus any of these models may be equivalently chosen if the purpose of the simulation is to analyse the product formed. Analysis of the batch reactor under the variation of the ratio of phenol and formaldehyde, $[\text{P}]_0/[\text{F}]_0$, in the feed shows that the maximum branching in the polymer occurs at a ratio of 0.5 whereas a ratio 1.60 is found to maximize the formation of linear chains. The application of a vacuum to the reaction mass has been modelled to give a constant but lower water concentration. The effect of the vacuum has been examined and is found to give a longer but more branched polymer compared with that for batch reactors with no vacuum.

Keywords Polymerization; novolac; phenol; formaldehyde; model; kinetics

INTRODUCTION

The condensation polymerization of phenol and formaldehyde in the presence of an acid catalyst is known to give an essentially linear polymer with little branching¹. The polymerization reaction has been schematically written as:



where $\begin{array}{c} \text{OH} \\ | \\ \text{C}_6\text{H}_4 \\ | \\ \text{OH} \end{array}$ indicates that the linkage could occur either at the *ortho* or *para* positions. Kinetically, the representation of the polymer formation through equation (1) is not correct because the *ortho* and *para* positions of the phenol exhibit different reactivities. In addition to this, Drumm *et al.*¹ pointed out the phenomena of molecular shielding in novolac formation, where the unreacted internal *ortho* and *para* positions on a given polymer molecule react at lower rates compared with the sites at the ends of the chain.

In our earlier studies²⁻⁴ on the modelling of novolac formation, various reactions were assumed to be completely irreversible. Molecules having at least two phenol rings were defined as polymer chains and the various sites on these chains, where polymerization can occur, were classified as: (a) *ortho* external O_{ef} ; (b) *para* external p_e ; (c) *ortho* internal O_i ; (d) *para* internal p_i . The above external sites are those which lie on the phenyl groups at the chain ends, whereas the internal sites are the remainder of the sites on the polymer chain. These sites were distinguished

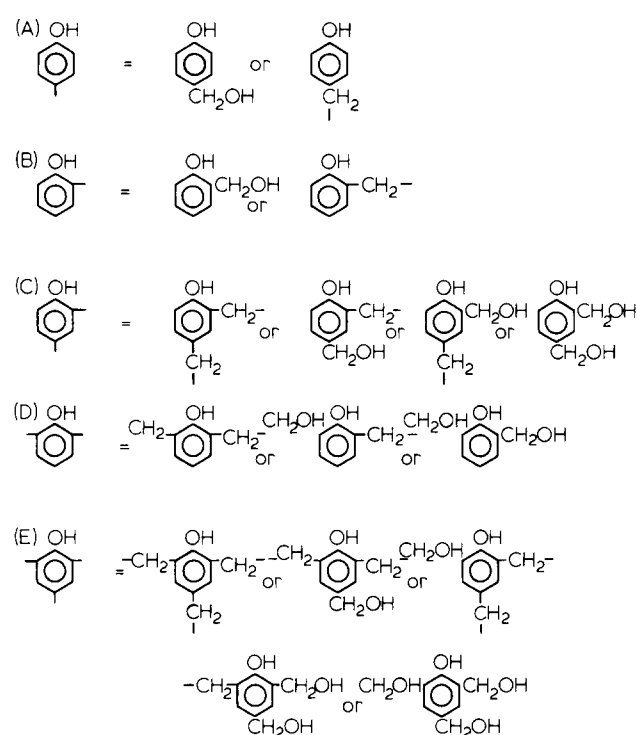
because they react with different rate constants. Mass balance equations for these were written using the general kinetics and solved numerically.

The earlier kinetic scheme, however, cannot be modified for the reversible polymerization of phenol formaldehyde. The difficulty arises because the reverse step involves a reaction between water and a $-\text{CH}_2-$ bond and the products formed depend on which groups lie on either side of the $-\text{CH}_2-$ linkage. An effort was made in this direction⁵ to write down the various types of bond linkages (thus distinguishing them) in the reaction mass, but this increases the number of species required to model the polymerization to thirty, an impractically high value.

In our earlier efforts to model the irreversible resole type polymerization^{6,7}, we proposed a kinetic model in which nineteen species were required. It was noted in a recent review⁸ that novolac formation can be equivalently described by the reaction between these nineteen species. Since this is a more detailed version of the earlier model²⁻⁴, an attempt was also made to extend it to describe the reversible novolac formation. An effort along this line, however, runs into difficulty because the reverse step for the formation of some of the species cannot be easily written.

In this paper we present a simple model for reversible novolac formation. We define five species A to E shown in Table 1. Here a dash on the benzene ring indicates either a $-\text{CH}_2-$ linkage or the presence of a $-\text{CH}_2\text{OH}$ group. In the same table, species A to E have been compared with the species defined in the work of Pal *et al.*^{6,7} Various reactions in the reversible polymerization have been written. While writing the reversible step, it was possible to have two possible routes of reaction and therefore there are two possible kinetic models 1 and 2 as shown in Table 2.

* To whom all correspondence should be addressed.

Table 1 Structure of various species used for the modelling of reversible novolac formation

Using kinetic models 1 and 2, mass balance equations for species A to E, phenol, formaldehyde and bound $-\text{CH}_2\text{OH}$ are written and numerically solved. Since these models represent the two asymptotes, the concentrations of these species in actual polymerization would lie between the two limits. The analysis shows that the concentrations of species A to E are identical for both the models whereas the concentrations of formaldehyde and bound CH_2OH are different. This means that either of these models could be used to predict the properties of the polymer formed.

Our earlier studies have shown the importance of unequal reactivity on the conversion and molecular weight distribution⁹⁻¹³. Here we have examined the effect of unequal reactivity on the reversible formation of the novolac. The ratio of phenol to formaldehyde, $[\text{P}]_0/[\text{F}]_0$, in the feed to the batch reactor shows that the formation of linear chains are maximized at about $[\text{P}]_0/[\text{F}]_0 = 1.60$. It is interesting to note that the industrially used ratio is 1.67.¹

KINETIC MODEL

To be able to model reversible novolac formation, the various reactions between species A to E given in *Table 1* are given in *Table 2*. In defining these species, the linkages with both CH_2OH and $-\text{CH}_2-$ have both been denoted by dashed lines on the phenyl rings. In the reaction mass, there are molecules of phenol and formaldehyde in addition to these species. Formaldehyde exists¹ as methylene glycol ($\text{OH}-\text{CH}_2-\text{OH}$) and the reaction of the OH group gives rise to bound CH_2OH which can further react to give the formation of a bond. Therefore the various forward reactions in *Table 2* have been divided into

reactions of different sites on P and A to E with formaldehyde (F) and bound CH_2OH . Since there are two groups on $\text{CH}_2(\text{OH})_2$, it reacts at twice the rate of reaction of bound CH_2OH .

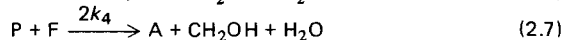
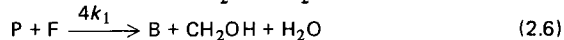
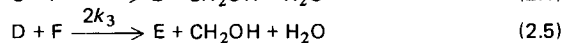
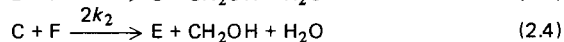
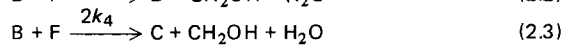
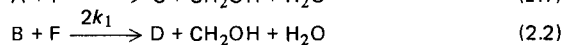
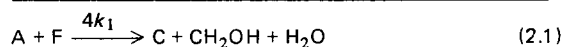
To write a general kinetic scheme accounting for molecular shielding in *Table 2*, four rate constants, k_1 for external *ortho*, k_2 for internal *ortho*, k_3 for internal *para* and k_4 for external *para* sites have been defined. In a given reaction, the overall reactivity is assumed to be completely determined by the site involved. Species A has two external *ortho* sites and whenever either of them is reacted

Table 2 Reaction mechanisms for model 1 and model 2

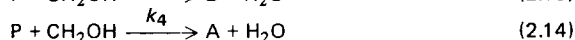
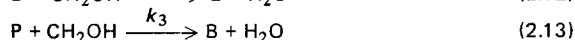
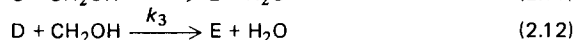
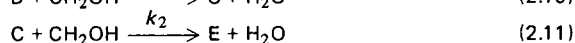
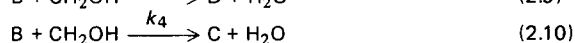
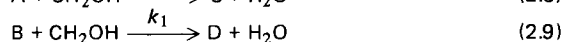
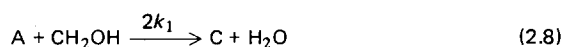
Model 1

(1) Forward reactions:

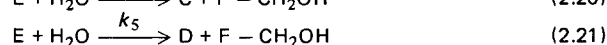
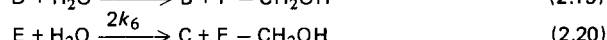
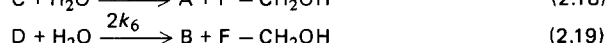
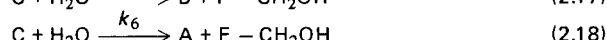
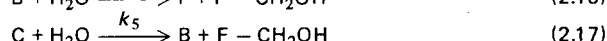
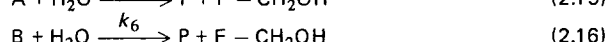
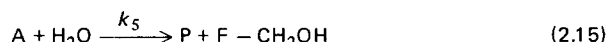
(i) Reactions with formaldehyde existing as methylene glycol



(ii) Reactions with $-\text{CH}_2\text{OH}$



(2) Reverse reactions:

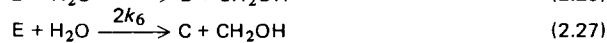
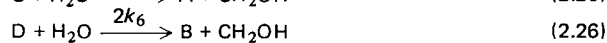


Model 2

(1) Forward reactions:

In model 2 forward reactions are same as in model 1; only the reverse reactions are different.

(2) Reverse reactions:



with F or CH₂OH (reactions (2.1) and (2.8) of Table 2), species C is formed. When the reaction with formaldehyde occurs, in addition to the formation of C, a bound CH₂OH group is also produced. Similarly B has one external *ortho* and one external *para* site, C has one internal *ortho* and D has one internal *para* site and their reactions are similarly written.

In the reverse reaction of novolac polymer molecules, water can interact with -CH₂- bonds as well as bound CH₂OH groups. To be able to write the mechanism of reaction of water with bonds, both the endings of the bond must be specified. In model 1 described in Table 2 the various link points on species A to E have been assumed to be largely CH₂OH. As a result when these react with water, formaldehyde (F) is formed with a loss of a bound CH₂OH group. This fact has been represented in equations (2.15) to (2.20) in Table 2 as (F-CH₂OH) on their right hand sides. This is done only for the purpose of book-keeping.

In model 2, also given in Table 2, the various link points have been assumed to be -CH₂- bonds. Consequently, when A to E react with H₂O in the reverse reaction, the reaction product is essentially -CH₂OH. Results for actual polymerizations would lie between these two limits of models 1 and 2. With these kinetic models, the mass balance equations for various species can be written for isothermal batch reactors as follows:

Model 1

$$\frac{d[A]}{dt} = 2k_4[P][F] - 4k_1[A][F] + k_4[P][CH_2OH] - 2k_1[A][CH_2OH] - k_5[A][H_2O] + k_6[C][H_2O] \quad (2)$$

$$\frac{d[B]}{dt} = 4k_1[P][F] - 2k_1[B][F] - 2k_4[B][F] + 2k_1[P][CH_2OH] - k_1[B][CH_2OH] - k_4[B][CH_2OH] - k_6[B][CH_2OH] + k_5[C][H_2O] + 2k_6[D][H_2O] \quad (3)$$

$$\frac{d[C]}{dt} = 4k_1[A][F] + 2k_4[B][F] - k_2[C][F] + 2k_1[A][CH_2OH] + k_4[B][CH_2OH] - k_2[C][CH_2OH] - k_5[C][H_2O] - k_6[C][H_2O] + 2k_6[E][H_2O] \quad (4)$$

$$\frac{d[D]}{dt} = 2k_1[B][F] - 2k_3[D][F] + k_1[B][CH_2OH] - k_3[D][CH_2OH] - 2k_6[D][H_2O] + k_5[E][H_2O] \quad (5)$$

$$\frac{d[E]}{dt} = 2k_2[C][F] + 2k_3[D][F] + k_2[C][CH_2OH] + k_3[D][CH_2OH] - 2k_6[E][H_2O] - k_5[E][H_2O] \quad (6)$$

$$\frac{d[F]}{dt} = -4k_1[A][F] - 2k_1[B][F] - 2k_1[B][F] - 2k_2[C][F] - 2k_3[D][F] - 4k_1[P][F] + 2k_4[P][F] + k_5[A][H_2O] + k_6[B][H_2O] + k_5[C][H_2O] + k_6[C][H_2O] + 2k_6[D][H_2O] + 2k_6[E][H_2O] + k_5[E][H_2O] \quad (7)$$

$$\frac{d[P]}{dt} = -4k_1[P][F] - 2k_4[P][F] - 2k_1[P][CH_2OH] - k_4[P][CH_2OH] + k_5[A][H_2O] + k_6[B][H_2O] \quad (8)$$

$$\frac{d[CH_2OH]}{dt} = 4k_1[A][F] + 2k_1[B][F] + 2k_4[B][F] + 2k_2[C][F] + 2k_3[D][F] + 4k_1[P][F] + 2k_4[P][F] - 2k_1[A][CH_2OH] - k_1[B][CH_2OH] - k_4[B][CH_2OH] - k_2[C][CH_2OH] - k_3[D][CH_2OH] - 2k_1[P][CH_2OH] - k_4[P][CH_2OH] - k_5[A][H_2O] - k_6[B][H_2O] - k_5[C][H_2O] - k_6[C][H_2O] - 2k_6[D][H_2O] - 2k_6[E][H_2O] - k_5[E][H_2O] \quad (9)$$

$$\frac{d[H_2O]}{dt} = 4k_1[A][F] + 2k_1[B][F] + 2k_4[B][F] + 2k_2[C][F] + k_3[D][F] + 4k_1[P][F] + 2k_4[P][F] + 2k_1[A][CH_2OH] + k_1[B][CH_2OH] + k_4[B][CH_2OH] + k_2[C][CH_2OH] + k_3[D][CH_2OH] + 2k_1[P][CH_2OH] + k_4[P][CH_2OH] - k_5[A][H_2O] - k_6[B][H_2O] - k_5[C][H_2O] - k_6[C][H_2O] - 2k_6[D][H_2O] - 2k_6[E][H_2O] - k_5[E][H_2O] \quad (10)$$

Model 2

For this kinetic model, only the reverse terms of the mass balance equations of F and CH₂OH change. The mass balance equations of other species are the same as for model 1.

$$\frac{d[F]}{dt} = -4k_1[A][F] - 2k_1[B][F] - 2k_4[B][F] - 2k_2[C][F] - 2k_3[D][F] - 4k_1[P][F] - 2k_4[P][F] \quad (11)$$

$$\frac{d[CH_2OH]}{dt} = 4k_1[A][F] + 2k_1[B][F] + 2k_4[B][F] + 2k_2[C][F] + 2k_3[D][F] + 4k_1[P][F] + 2k_4[P][F] - 2k_1[A][CH_2OH] - k_1[B][CH_2OH] - k_4[B][CH_2OH] - k_2[C][CH_2OH] - k_3[D][CH_2OH] - 2k_1[P][CH_2OH] - k_4[P][CH_2OH] + k_5[A][H_2O] + k_6[B][H_2O] + k_5[C][H_2O] + k_6[C][H_2O] + 2k_6[D][H_2O] + 2k_6[E][H_2O] + k_5[E][H_2O] \quad (12)$$

Equations (2) to (12) were rearranged and written in terms of the following dimensionless groups:

$$x = k_1 t [F]_0$$

$$R_1 = k_2/k_1; \quad R_2 = k_3/k_1; \quad R_3 = k_4/k_1;$$

$$R_4 = k_5/k_1; \quad R_5 = k_6/k_1$$

$$y_1 = [A]/[F]_0$$

$$y_2 = [B]/[F]_0$$

$$\begin{aligned}
 y_3 &= [C]/[F]_0 \\
 y_4 &= [D]/[F]_0 \\
 y_5 &= [E]/[F]_0 \\
 y_6 &= [F]/[F]_0 \\
 y_7 &= [P]/[F]_0 \\
 y_8 &= [\text{CH}_2\text{OH}]/[F]_0 \\
 y_9 &= [\text{H}_2\text{O}]/[F]_0
 \end{aligned}$$

Equations (2) to (12) are coupled nonlinear differential equations and are solved using the Runge-Kutta method of fourth order with Δx as 10^{-3} .

RESULTS AND DISCUSSION

To check the numerical stability of the solution, the time increment Δx was changed from 10^{-3} to 10^{-5} and the same concentration profiles of the various species were obtained. In addition to this, in all computations, the ring count defined by

$$\text{Ring count} = [P] + [A] + [B] + [C] + [D] + [E] \quad (13)$$

was calculated. This should remain constant, which was indeed found to be so in all computations.

Our earlier studies have shown that the irreversible formation of novolac is insensitive to the phenomena of molecular shielding. As a result, the following approximation has been made in this simulation study

$$R_1 = 1 \quad (14a)$$

$$R_2 = R_3 \quad (14b)$$

In addition to this, the reverse step involves two rate constants, k_5 to k_6 . Since the *ortho* and *para* positions in the forward reaction exhibit different reactivities, they are assumed to differ in the reactivity by the same ratio in the reverse step. This would mean that

$$\frac{R_4}{R_5} = R_3 \quad (15)$$

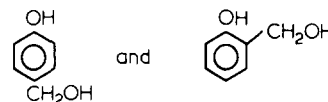
In the absence of any information on the equilibrium of phenol formaldehyde polymerization, R_5 has been taken as a parameter in this study. The concentrations of species A to E, phenol, formaldehyde, bound CH_2OH and water have been calculated for models 1 and 2 for various values of R_5 . It was found that for both these models, [A], [B], [C], [D], [E], [P] and $[\text{H}_2\text{O}]$ versus time remained the same for any given set of rate constants. This appears to be surprising on the first hand. It may be noted that models 1 and 2 differ only in the reverse reactions and the terms in the balance equations for $[\text{CH}_2\text{OH}]$ and $[F]$ are different for these two models. For other species, however, the change in the model is supposed to have an indirect effect through the concentrations of F and CH_2OH in the reaction mass. It is further observed that whenever a functional group OH reacts, one molecule of water is formed. As a result, at any time of polymerization, the following relation would hold:

$$2[F] + [\text{CH}_2\text{OH}] + [\text{H}_2\text{O}] = 2[F]_0 \quad (16)$$

where the feed to the reactor is assumed to be a mixture of $[P]_0$ moles of phenol and $[F]_0$ moles of formaldehyde

only. In equations (2) to (10), the terms involving concentrations of formaldehyde and bound CH_2OH always appear together as $(2[F] + [\text{CH}_2\text{OH}])$. Through equations (7) and (8) for model 1 and equations (11) and (12) for model 2, it can be shown that the rate of change of $(2[F] + [\text{CH}_2\text{OH}])$ is the same for both the models.

In our earlier model of irreversible novolac formation, we had used the various reaction sites (O'_o , O_o , O_i and p_o) on polymer chains having chain length of two units and more. The results presented therein cannot be directly compared with the results obtained here for irreversible polymerization because in models 1 and 2 we have included species of unit chain length (excluding phenol) as polymer molecules. On adding concentrations of



to the results of various site concentrations obtained from the earlier studies^{2,3}, results of this work are found to be consistent.

In Figures 1 to 7, y_1 to y_7 have been plotted as a function of the dimensionless time, x , with R_5 as parameter. $(2[A] + [B])$ gives the total concentration of external *ortho* sites in the reaction mass and has been plotted in Figure 1. For a given R_5 , the curve rises very quickly but falls only very slightly at longer times. As R_5 is increased from 0.0 to 1.0, the change in these curves is only very slight; however for values of R_5 higher than this, the fall in the numerical value is large indicating that the polymerization has not proceeded to any extent. A similar fall in C versus x in Figure 2, D versus x in Figure 3 and E versus x in Figure 4 confirms the decrease in chain length of the polymer formed as R_5 is increased to a large value. As shown in Figure 5, the asymptotic value of unreacted phenol in the reaction mass with R_5 increases accordingly. In our earlier studies of irreversible formation, we found that the concentrations of various sites first increased reaching an asymptotic value for large times. This behaviour was found to be so because all the formaldehyde and bound $-\text{CH}_2\text{OH}$ are completely reacted. In the reversible novolac formation, we find the same behaviour, except for the fact that the curves reach the asymptotic value because of the equilibrium. As R_5 is increased, the polymer formation reduces and the asymptotic values for curves for [A] to [E] versus x fall.

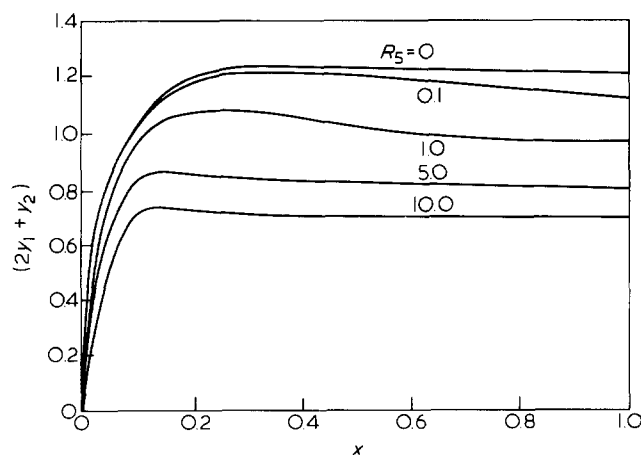


Figure 1 Effect of R_5 on $(2[A] + [B])$ versus x . $R_1 = 1$, $R_2 = R_3 = 2.4$, $R_4 = 2.4$, R_5 , $[P]_0/[F]_0 = 1.67$

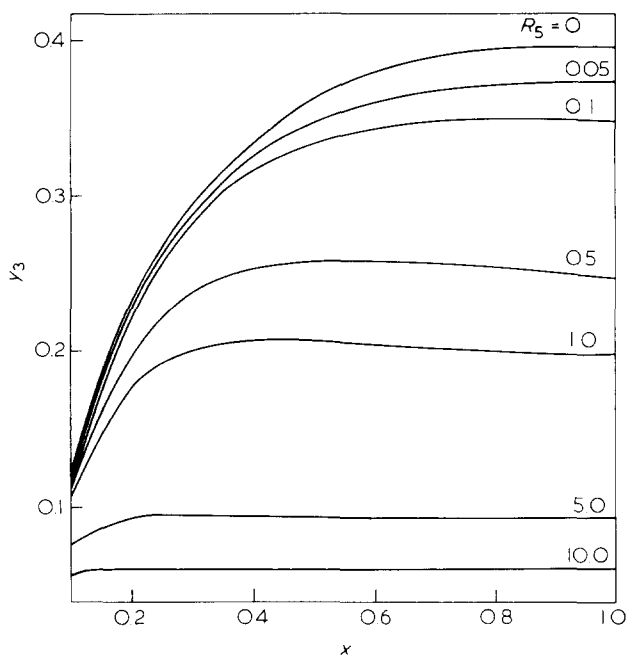


Figure 2 Effect of R_5 on [C] versus x . $R_1 = 1, R_2 = R_3 = 2.4, R_4 = 2.4 R_5, [P]_0/[F]_0 = 1.67$

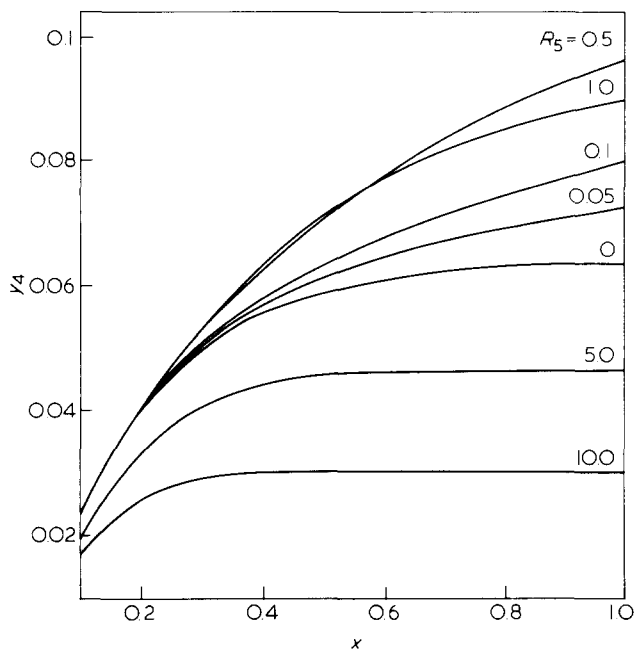


Figure 3 Effect of R_5 on [D] versus x . $R_1 = 1, R_2 = R_3 = 2.4, R_4 = 2.4 R_5, [P]_0/[F]_0 = 1.67$

The concentrations of formaldehyde and bound CH_2OH versus dimensionless time x for both models 1 and 2 are given in Figures 6 and 7 respectively. For model 1, $[\text{F}]$ approaches an asymptotic value for large values x , which increases as R_5 is increased; for Model 2, however, as expected, the effect of R_5 is very small. In Figure 7, $[\text{CH}_2\text{OH}]$ has been plotted as a function of x and is found to undergo a maximum before going to zero for longer times. For model 1, the maximum value of $[\text{CH}_2\text{OH}]$ reduces whereas for model 2, the maximum disappears for values of R_5 greater than 1.

In Figures 8 to 11, the effect of the phenol to formaldehyde ratio in the feed, $[\text{P}]_0/[\text{F}]_0$, on the con-

centration of various species has been examined. These computational runs were made with $[\text{F}]_0 = 1$ and varying $[\text{P}]_0$ in the feed. Thus the upward increasing trend in Figure 8 for $2[\text{A}] + [\text{B}]$ with increasing $[\text{P}]_0/[\text{F}]_0$ exists because more and more phenol molecules give a larger number of external *ortho* sites. A similar trend in $[\text{C}]$ and $[\text{D}]$ is found in Figures 9 and 10 respectively. However for $[\text{P}]_0/[\text{F}]_0$ beyond 1.6, both $[\text{C}]$ and $[\text{D}]$ begin to fall. It may be noted that the increase in $[\text{C}]$ and $[\text{D}]$ indicates the increase in linear polymer molecules of chain length of 3 units and more. Thus $[\text{P}]_0/[\text{F}]_0 = 1.60$ maximizes the formation of linear chains. It is interesting to note that commercial novolac reactors are operated at the feed ratio of 1.67. In Figure 11, the effect of $[\text{P}]_0/[\text{F}]_0$ in the feed on $[\text{E}]$ versus x has been examined. As this ratio is increased, $[\text{E}]$ versus x curves rise to higher values and for the ratio beyond 0.5 it begins to fall. A large concentration of species E in the reaction mass indicates that the

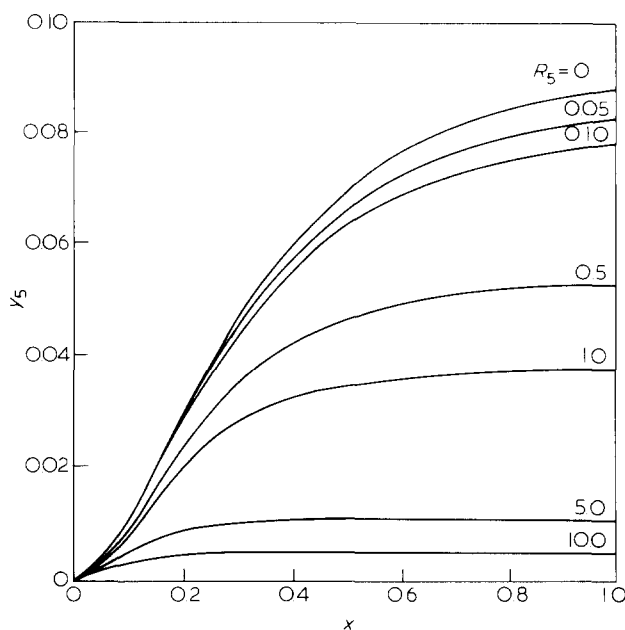


Figure 4 Effect of R_5 on E versus x . $R_1 = 1, R_2 = R_3 = 2.4, R_4 = 2.4 R_5, [P]_0/[F]_0 = 1.67$

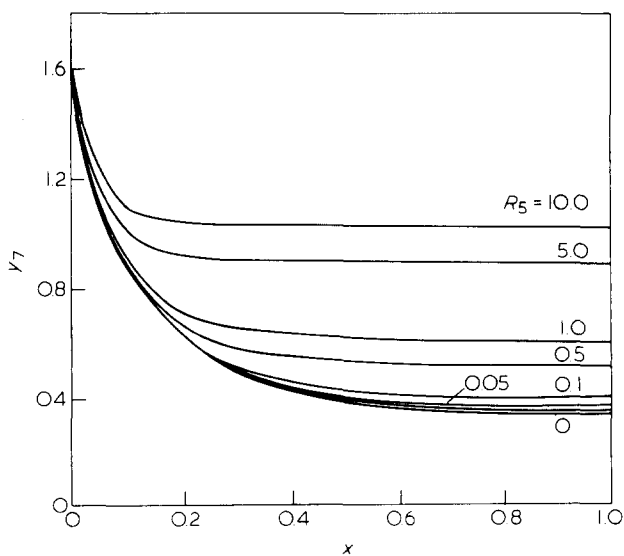


Figure 5 Effect of R_5 on [P] versus x . $R_1 = 1, R_2 = R_3 = 2.4, R_4 = 2.4 R_5, [P]_0/[F]_0 = 1.67$

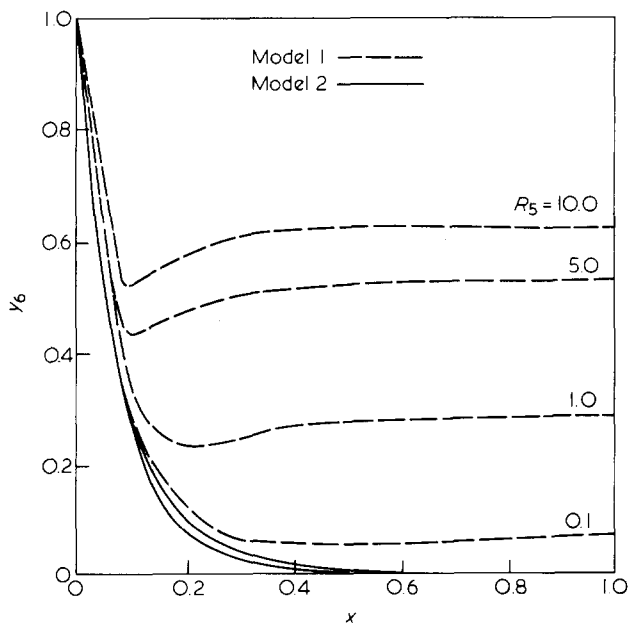


Figure 6 Effect of R_5 on $[F]$ versus x for model 1 and 2. $R_1 = 1$, $R_2 = R_3 = 2.4$, $R_4 = 2.4 R_5$, $[P]_0/[F]_0 = 1.67$

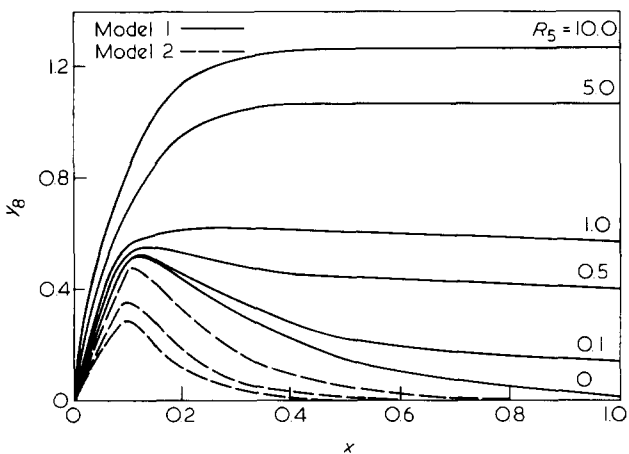


Figure 7 Effect of R_5 on $[CH_2OH]$ versus x for models 1 and 2. $R_1 = 1$, $R_2 = R_3 = 2.4$, $R_4 = 2.4 R_5$, $[P]_0/[F]_0 = 1.67$

polymer formed is branched. This would mean that $[P]_0/[F]_0 = 0.5$ would lead to the highest branching which is consistent with our earlier studies of resole formation^{6,8}. Indeed, resole polymerizations are usually carried out at these values of $[P]_0/[F]_0$.

In the computation of Figures 1 to 11, the water as the condensation product is assumed to remain in one phase during the polymerization. When a vacuum is applied on the reaction mass, the water concentration falls and the rate of polymerization is expected to increase. A concentration profile of water is established which can, in general, be solved through differential mass transfer equations^{14,15}. For most applications where the gel point is not reached, the mass transfer resistance is small, as a result of which, the concentration of water can be assumed to be uniform in the reaction mass given by the vapour liquid equilibrium existing at the pressure applied^{16,17}. In Figures 12 to 14, we have considered the concentration of water in the reaction mass as a parameter and compared the results with the results of batch reactors where water is

not removed. In Figures 12, 13 and 14, the effect of $[H_2O]$ level (i.e., the vacuum applied) on $(2[A] + [B])$, $[C]$ and $[E]$ versus x has been examined. As the concentration level of H_2O is reduced, these curves shift upwards; however, the effect on $(2[A] + [B])$ versus x is relatively small. For the same residence time, on application of a vacuum, this means that the branching and the length of the polymer formed is increased.

CONCLUSION

Reversible novolac formation has been modelled through the five reactive species A to E. These differ from each other only in terms of their reacted sites. A given site on

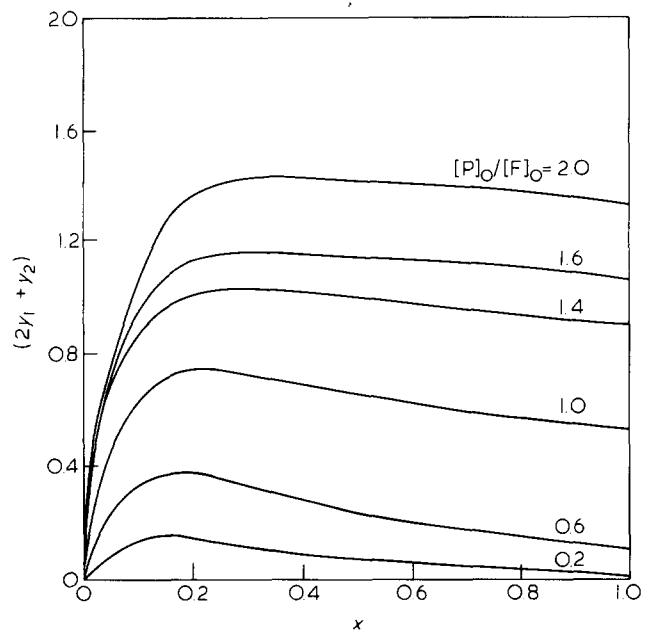


Figure 8 Effect of $[P]_0/[F]_0$ on $(2[A] + [B])$ versus x . $R_1 = 1$, $R_2 = R_3 = 2.4$, $R_4 = 0.24$, $R_5 = 0.1$

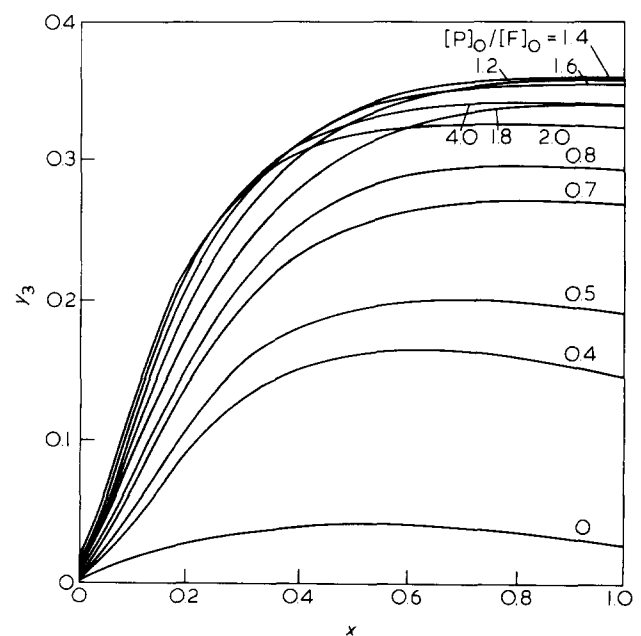


Figure 9 Effect of $[P]_0/[F]_0$ on $[C]$ versus x . $R_1 = 1$, $R_2 = R_3 = 2.4$, $R_4 = 0.24$, $R_5 = 0.1$

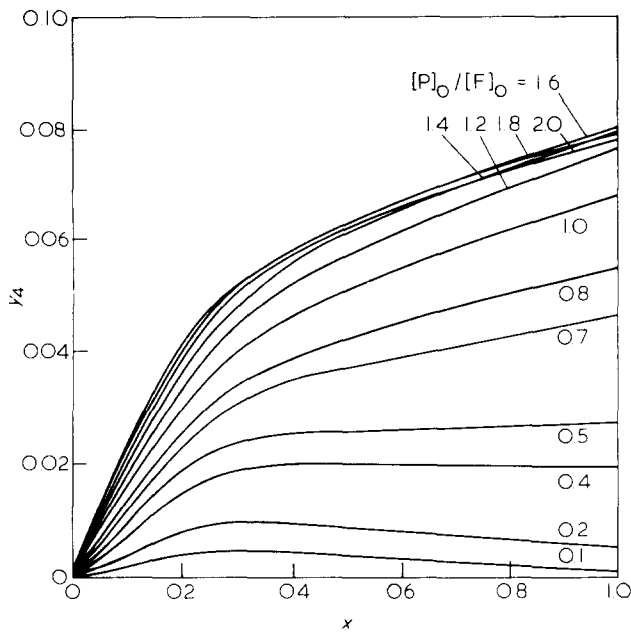


Figure 10 Effect of $[P]_0/[F]_0$ on $[D]$ versus x . $R_1 = 1, R_2 = R_3 = 2.4, R_4 = 0.24, R_5 = 0.1$

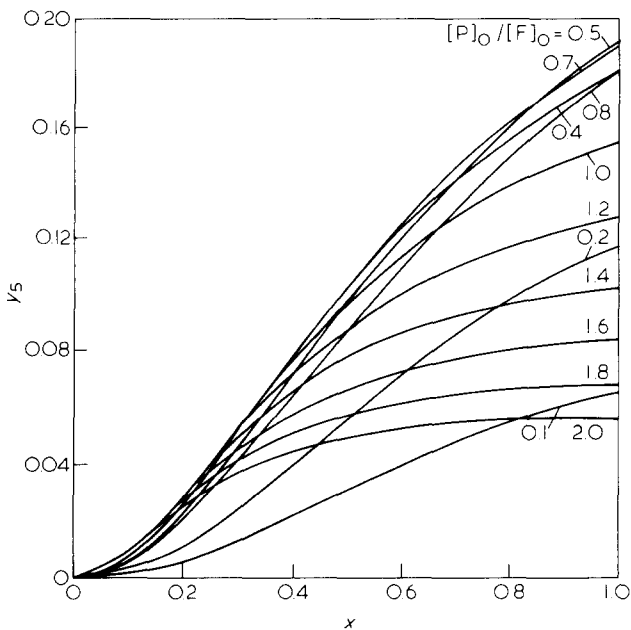


Figure 11 Effect of $[P]_0/[F]_0$ on E versus x . $R_1 = 1, R_2 = R_3 = 2.4, R_4 = 0.24, R_5 = 0.1$

these species could either be connected through a $-\text{CH}_2-$ bond or just be simply linked to a CH_2OH group.

Depending upon whether the linkages on species A to E are predominantly $-\text{CH}_2-$ bonds or CH_2OH , it is possible to write two asymptotic kinetic models 1 and 2. The analysis of these models show that both predict identical characteristics of the polymer formed whereas an uncertainty exists in predicting $[F]$ and $[\text{CH}_2\text{OH}]$ in the reaction mass.

For predicting the nature of the polymer formed, either of the models 1 and 2 could be chosen to examine the effect of reverse rate constant and the ratio of phenol and formaldehyde, $[P]_0/[F]_0$, model 1 has been used for the analysis. Our earlier analyses have shown that molecular shielding has only a very small influence on the character-

istics of the polymer formed, in view of which, the internal and external *ortho* and *para* sites have not been distinguished kinetically here. In the reverse reaction the *para* linkages are assumed to react with water with higher rate constants compared with that for *ortho* linkages. The effect of increasing the reverse rate constant is to reduce the polymer chains, as expected.

Increasing the ratio $[P]_0/[F]_0$ in the feed leads to an increased branching which undergoes a maximum at $[P]_0/[F]_0 \approx 0.5$. When this ratio is increased further, the degree of branching falls but, the concentrations of internal sites (whose measure is indicated by $[C]$ and $[D]$) in the reaction mass undergoes a maximum at

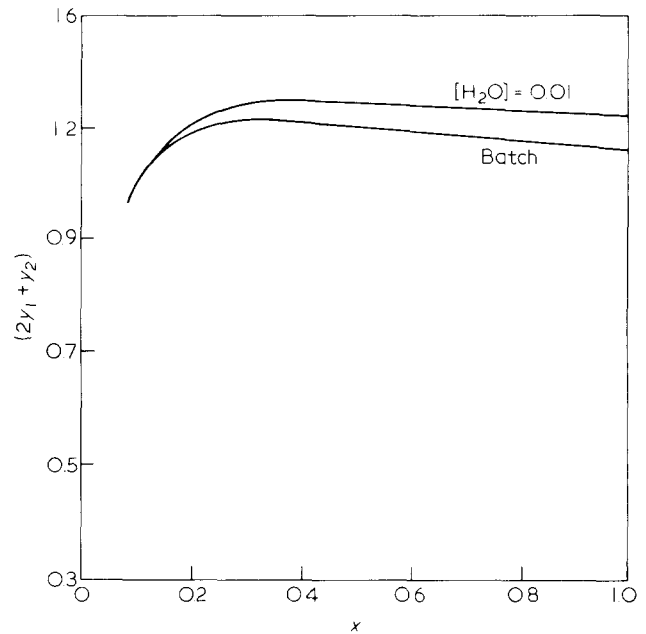


Figure 12 Effect of vacuum on $(2[A] + [B])$ versus x . $R_1 = 1, R_2 = R_3 = 2.4, R_4 = 0.24, R_5 = 0.1, [P]_0/[F]_0 = 1.67$

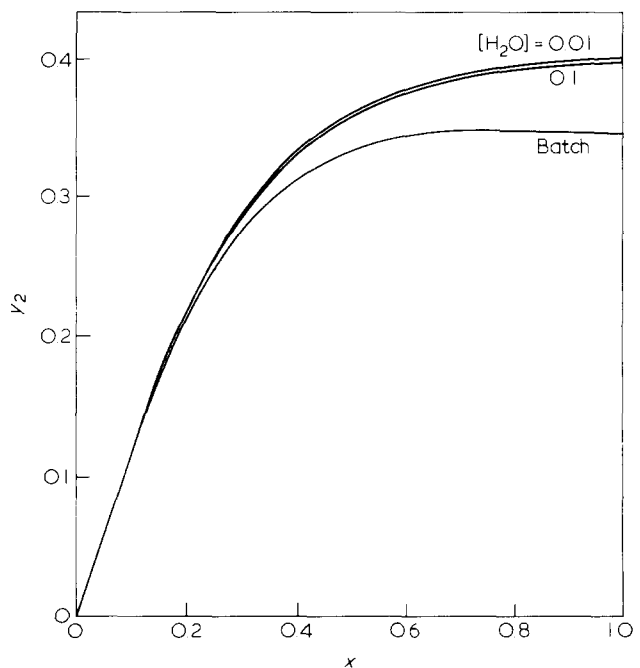


Figure 13 Effect of vacuum on $[C]$ versus x . $R_1 = 1, R_2 = R_3 = 2.4, R_4 = 0.24, R_5 = 0.1, [P]_0/[F]_0 = 1.67$

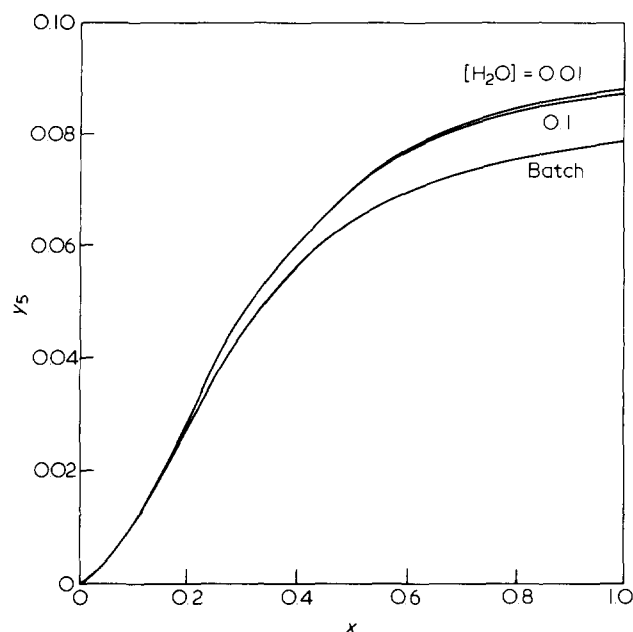


Figure 14 Effect of vacuum on $[E]$ versus x . $R_1 = 1, R_2 = R_3 = 2.4, R_4 = 0.24, R_5 = 0.1, [P]_0/[F]_0 = 1.67$

$[P]_0/[F]_0 = 1.60$. This maximum in $[C]$ and $[D]$ implies the preponderance of linear polymer chains with chain lengths of 3 units and more. Interestingly enough, industrially, reactors producing novolac polymer, where the aim is to maximize the production of linear chains, are operated with $[P]_0/[F]_0 = 1.67$.

The effect of application of vacuum on the novolac polymer formed has also been examined by assuming a constant water concentration in the reaction mass. As water is reduced through the application of vacuum, a longer and more highly branched polymer is formed.

REFERENCES

- 1 Drumm, M. F. and LeBlanc, J. R. in 'Step Growth Polymerization, (Ed. D. H. Solomon), 1st Edn., Marcel Dekker, New York, 1972
- 2 Kumar, A., Kulshreshtha, A. K. and Gupta, S. K. *Polymer* 317, 21, 1980
- 3 Kumar, A., Gupta, S. K. and Kulshreshtha, A. K. and Phukan, U. K. *Polymer* 1982, 23, 215
- 4 Kumar, A., Gupta, S. K. and Phukan, U. K. *Polym. Eng. Sci.* 1218, 21, 1981
- 5 Phukan, U. K., *M.Tech. Thesis*, Department of Chemical Engineering, Indian Institute of Technology, Kanpur, 1980
- 6 Gupta, S. K., Kumar, A. and Pal, P. K. *Br. Polym. J.* 121, 12, 1980
- 7 Pal, P. K., Kumar, A. and Gupta, S. K. *Polymer* 1981, 22, 1699
- 8 Gupta, S. K. and Kumar, A. *Chem. Eng. Commun.* in press
- 9 Goel, R., Gupta, S. K. and Kumar, A. *Polymer*, 1977, 18, 851
- 10 Gupta, S. K., Kumar, A. and Bhargava, A. *Eur. Polym. J.* 1979, 15, 557
- 11 Gupta, S. K., Kumar, A. and Bhargava, A. *Polymer* 1979, 20, 305
- 12 Gupta, S. K., Agarwalla, N. L., Rajora, P. and Kumar, A. *J. Polym. Sci., Polym. Phys. Edn.*, in press
- 13 Kumar, A., Rajora, P., Agarwalla, N. L. and Gupta, S. K. *Polymer* 1982, 23, 222
- 14 Gupta, S. K., Agarwalla, N. L. and Kumar, A. *J. Appl. Polym. Sci.*, in press
- 15 Gupta, S. K., Kumar, A., Agarwal, K. K. *Polymer* 1982, 23, 1367
- 16 Kumar, A., Gupta, S. K. and Somu, N. *Polym. Eng. Sci.* 1982, 22, 314
- 17 Kumar, A., Gupta, S. K. and Gupta, B. *J. Appl. Polym. Sci.*, in press